

# Semi-classical and boson descriptions of scissors states

A. A. Raduta<sup>a),b)</sup>, C. M. Raduta<sup>a)</sup> and Robert Poenaru<sup>c)</sup> and Al. H. Raduta<sup>a)</sup>

<sup>a)</sup> Department of Theoretical Physics, Institute of Physics and Nuclear Engineering, Bucharest, POBox MG6, Romania

<sup>b)</sup> Academy of Romanian Scientists, 54 Splaiul Independentei, Bucharest 050094, Romania and

<sup>c)</sup> Department of Inovation, Orange Services, Str. Gara Herastrau 4D, Bucharest, Romania

A two-rotors Hamiltonian is alternatively treated semi-classically and by a Dyson boson expansion method. The linearized equations of motion lead to dispersion equation for the wobbling frequency. One defined a ground band with energies consisting in a rotational part and a zero-point energy. Adding to each state energy the corresponding wobbling quanta one obtains the first excited band. Phonon amplitudes are used to calculate the reduced probability for the interband M1 transition. The states initially exhibit a shears character but as rotational alignment progresses, they gradually evolve to a scissors-like configuration. One points out a chiral symmetry which is broken by an addition interaction term, leading to a twin pair of chiral bands. Applications are made for  $^{156}\text{Gd}$ . One outlines the ability of the two rotor model to account for the wobbling and chiral motion in nuclei.

PACS numbers: 21.10.Ky, 21.10.Re, 21.60.Ev

## I. INTRODUCTION

The description of magnetic properties in nuclei has always been a central issue. The reason is that the two systems of protons and neutrons respond differently when they interact with an external electromagnetic field. Differences are due to the fact that by contrast to neutrons, protons are charged particles, the proton and neutron magnetic moments are different from each other and finally the protons and neutron numbers are also different. It was in 1965 that Greiner and his collaborators advanced the idea about different moments of inertia for proton and neutron systems [1] which should be reflected both in energies and magnetic transitions. This idea was further elaborated under the name of the two liquid drops model which has been used to describe the isovector  $2^+$  state [2] as well as the M1 properties [3] of the rotational bands. Few years later a microscopic description of the magnetic dipole states was proposed by Gabrakov, Kuliev and Pyatov [4], by using a deformed Woods Saxon mean field for the single particle motion. Shortly after, the same authors succeeded to eliminate the isoscalar spurious contributions to the magnetic mode [5]. Such dipole excitation was also studied by Rowe [6] within the potential vibrating method. The group which brought something essentially new in this field is that of Lo Iudice and Palumbo [7]. They developed a phenomenological model, called Two Rotor Model (TRM), which assigns to the proton and neutron systems two rigid rotors, which are axially symmetric with different symmetry axes. The mode appears to be a vibrational mode of the angle between the two symmetry axes. This picture inspired the naming as “scissors mode”. An essential property of the mode, predicted by TRM, is that it is excited due to the interaction of the nuclear convection current with the electromagnetic field. Although the predictions of the TRM for both energy and M1 probability to be excited, are much larger than the experimental data, obtained few years later, the big merit of this model is to predict a pure orbital mode, which is of collective nature, without involving the spin degrees of freedom. As a matter of fact, this feature was confirmed by all microscopic calculations. The field of collective M1 states was enormously stimulated by the group of Richter, which identified the M1 state, for  $^{156}\text{Gd}$ , in a high resolution ( $e, e'$ ) experiment at backward angles [8]. The results for the excitation energy and the  $B(\text{M1})$  value were confirmed by a nuclear resonance fluorescent experiment [9]. Since then, many experiments have been performed and the number of nuclei known to exhibit a scissors mode was enlarged by many rear-earth and actinides nuclei but also by some medium mass isotopes from the Ti region. Another phenomenological model aimed at describing the measured properties of  $1^+$  is the interacting boson model (IBA2). In this model, the M1 state is caused by breaking the F spin symmetry by a Majorana interaction of the proton-like and neutron-like bosons. The state energy is obtained by a suitable fixing of the interaction strength. Therefore IBA2 is not making predictions for the state energy but only for the M1 excitation probability from the ground state [10]. The generalized coherent state model (GCSM) [11] has been used to describe simultaneously the scissors mode and the first three major collective bands, ground,  $\beta$  and  $\gamma$ . The important finding of the proposed model is that the total M1 strength is proportional to the nuclear deformation squared, which proves the collective nature of the mode [12]. The first calculations and predictions for the scissors mode in even-odd nuclei were achieved in Refs. [13, 14].

To obtain more detailed information about the literature devoted to this subject, we advise the reader to consult the review papers on this issue [15–17].

Here we study the magnetic properties of scissors-like states within a two rotors model. We present a new view on this issue namely a two-rotor Hamiltonian, described in Section 2, is successively treated through a semi-classical and boson expansion procedures. These objectives are touched in sections 3 and 4, respectively. In these sections

the wobbling frequencies for a two rotor system are obtained. In Section 5 the expressions for the magnetic dipole reduced probabilities are derived. An extensive numerical analysis is presented in Section 6. One defines a ground and an excited wobbling band are defined whose energies are subsequently calculated. Also the corresponding B(M1) values for exciting states from the second the second band are calculated. The nature of the found states, scissors or shears, is investigated. Final conclusions are drown in Section 7.

## II. TWO ROTORS HAMILTONIAN

The objective of this paper is to study the properties of the following two rotors Hamiltonian:

$$H = \frac{\vec{I}_p^2}{2\mathcal{J}_p} + \frac{\vec{I}_n^2}{2\mathcal{J}_n}. \quad (2.1)$$

with  $\vec{I}_p$  and  $\vec{I}_n$  denoting the angular momenta carried by the proton and neutron system, respectively. The moments of inertia for the two systems, which are supposed to be axially deformed ellipsoids, are denoted by  $\mathcal{J}_p$  and  $\mathcal{J}_n$ , respectively.

For what follows it is useful to change the proton and neutron angular momenta through the transformation:

$$\begin{aligned} \vec{I} &= \vec{I}_p + \vec{I}_n \\ \vec{S} &= \vec{I}_p - \vec{I}_n. \end{aligned} \quad (2.2)$$

With the notation:

$$A_p = \frac{1}{2\mathcal{J}_p}, \quad A_n = \frac{1}{2\mathcal{J}_n}, \quad (2.3)$$

the Hamiltonian gets the form:

$$H = \frac{A_p + A_n}{4}(\vec{I}^2 + \vec{S}^2) + \frac{A_p - A_n}{4}[(I_+S_- + I_-S_+ + 2I_3S_3)], \quad (2.4)$$

where:

$$I_{\pm} = I_1 \pm I_2, \quad S_{\pm} = S_1 \pm S_2, \quad (2.5)$$

with  $I_k$ ,  $S_k$  with  $k=1,2,3$ , being the k-th Cartesian components of the vectors  $\vec{I}$ ,  $\vec{S}$ , respectively.

## III. SEMI-CLASSICAL DESCRIPTION

The main spectroscopic properties of  $H$  will be evidenced by the Time Dependent Variational Principle:

$$\delta \int \langle \Psi_{M\sigma}^{IS} | (H - i\frac{\partial}{\partial t'}) | \Psi_{M\sigma}^{IS} \rangle dt' = 0. \quad (3.1)$$

If the trial function spans the whole Hilbert space generated by the eigenfunction of  $H$ , then solving the variational equation is equivalent with solving the time dependent Schrödinger equation. Clearly  $H$  commutes with  $\vec{I}^2$  and  $\vec{S}^2$  but not with  $I_z$  and  $S_z$ , respectively. This suggests the following trial function, as a good candidate for the variational function:

$$\Psi_{M\sigma}^{IS} = \mathcal{N} e^{zI_-} e^{xS_-} |IMI\rangle |S\sigma S\rangle. \quad (3.2)$$

with  $z$  and  $x$  being complex functions of time playing the role of classical phase space coordinates. The term  $\mathcal{N}$  is the normalization factor:

$$\mathcal{N} = [(1 + |z|^2)(1 + |x|^2)]^{-1/2}, \quad (3.3)$$

while the states  $|IMI\rangle$  and  $|S\sigma S\rangle$  are defined as follows:

$$\begin{aligned} |IMI\rangle &= \sqrt{\frac{2I+1}{8\pi^2}} D_{MI}^{I*} \\ |S\sigma S\rangle &= \sqrt{\frac{2S+1}{8\pi^2}} D_{\sigma S}^{S*}. \end{aligned} \quad (3.4)$$

Throughout this paper the units where  $\hbar = c = 1$  are used.

Obviously, the function  $\Psi_{M\sigma}^{IS}$  is a linear combination of the vector states  $|IMK\rangle|S\sigma\kappa\rangle$  with the amplitudes close to those obtained through diagonalization procedure [18]. The average value of the partial time derivative has the expression:

$$\langle \frac{\partial}{\partial t} \rangle = IS \frac{\dot{z} z^* - z \dot{z}^*}{1 + |z|^2} \frac{\dot{x} x^* - x \dot{x}^*}{1 + |x|^2} \quad (3.5)$$

In order to get the average of  $H$  with the trial function defined above, we need the matrix elements of the raising and lowering operators:

$$\begin{aligned} \langle \hat{I}_- \rangle &= \mathcal{N}_z^2 \frac{\partial}{\partial z} (\mathcal{N}_z^{-2}) = \frac{2Iz^*}{1 + zz^*}, \\ \langle \hat{I}_+ \rangle &= \mathcal{N}_z^2 \frac{\partial}{\partial z^*} (\mathcal{N}_z^{-2}) = \frac{2Iz}{1 + zz^*}, \\ \langle \hat{S}_- \rangle &= \mathcal{N}_x^2 \frac{\partial}{\partial x} (\mathcal{N}_x^{-2}) = \frac{2Sx^*}{1 + xx^*}, \\ \langle \hat{I}_+ \rangle &= \mathcal{N}_x^2 \frac{\partial}{\partial x^*} (\mathcal{N}_x^{-2}) = \frac{2Sx}{1 + xx^*}, \end{aligned} \quad (3.6)$$

The normalization factors have the expressions:

$$N_z = (1 + |z|^2)^{-1/2}, \quad N_x = (1 + |x|^2)^{-1/2} \quad (3.7)$$

Also, it is easy to calculate the averages of the 3rd components of the vectors  $\vec{I}$  and  $\vec{S}$ :

$$\begin{aligned} \langle \hat{I}_3 \rangle &= I - z \langle \hat{I}_- \rangle = I - \frac{2Izz^*}{1 + zz^*}, \\ \langle \hat{S}_3 \rangle &= S - x \langle \hat{S}_- \rangle = S - \frac{2Sxx^*}{1 + xx^*}. \end{aligned} \quad (3.8)$$

Using the above equations, one obtains:

$$\langle \hat{I}_3^2 \rangle = \langle (\hat{I}_3 - z \hat{I}_-) (I - z \hat{I}_-) \rangle = I^2 - \frac{2I(2I-1)zz^*}{(1 + zz^*)^2}. \quad (3.9)$$

Averages for the components 1 and 2 of the angular momentum are obtained by combining the expressions listed above:

$$\begin{aligned} \langle \hat{I}_1^2 \rangle &= \frac{1}{4} \left[ 2I + \frac{2I(2I-1)}{(1 + zz^*)^2} (z + z^*)^2 \right], \\ \langle \hat{I}_2^2 \rangle &= -\frac{1}{4} \left[ -2I + \frac{2I(2I-1)}{(1 + zz^*)^2} (z - z^*)^2 \right]. \end{aligned} \quad (3.10)$$

It is worth mentioning the fact that the averages of angular momenta square are  $I(I+1)$  and  $S(S+1)$  respectively

$$\begin{aligned} \langle \hat{I}_1^2 \rangle + \langle \hat{I}_2^2 \rangle + \langle \hat{I}_3^2 \rangle &= I(I+1), \\ \langle \hat{S}_1^2 \rangle + \langle \hat{S}_2^2 \rangle + \langle \hat{S}_3^2 \rangle &= S(S+1). \end{aligned} \quad (3.11)$$

These equations reflect the fact that  $\Psi(z)_{M,\sigma}^{IS}$  is an eigenfunction for both  $\hat{I}^2$  and  $\hat{S}^2$ .

For what follows it is convenient to use the polar form for the classical coordinates  $z$  and  $x$ :

$$z = \rho e^{i\varphi}, \quad x = \nu e^{i\psi}. \quad (3.12)$$

Also, we change the variables  $\rho$  and  $\nu$  to:

$$r = \frac{2I}{1 + \rho^2}, \quad t = \frac{2S}{1 + \nu^2} \quad (3.13)$$

In terms of the new coordinates the classical energy function is:

$$\begin{aligned} \langle \Psi_{M\sigma}^{IS} | H | \Psi_{M\sigma}^{IS} \rangle &\equiv \mathcal{H} = \mathcal{H}_0 + \mathcal{H}_1, \quad \text{where} \\ \mathcal{H}_0 &= A_+ (I(I+1) + S(S+1)) + A_- (I-1)(S-1), \\ \mathcal{H}_1 &= 2A_- \sqrt{rt(2I-r)(2S-t)} \cos(\psi - \varphi) + A_- \left[ \frac{I-1}{2S}t + \frac{S-1}{2I}r + \frac{rt}{4IS} \right]. \end{aligned} \quad (3.14)$$

with the notation

$$A_{\pm} = \frac{A_p \pm A_n}{4}. \quad (3.15)$$

The time dependent variational equation yields the classical equations of motion, which are of canonical Hamilton form:

$$\begin{aligned} \frac{\partial \mathcal{H}}{\partial r} &= \dot{\varphi}, \quad \frac{\partial \mathcal{H}}{\partial \varphi} = -\dot{r}, \\ \frac{\partial \mathcal{H}}{\partial t} &= \dot{\psi}, \quad \frac{\partial \mathcal{H}}{\partial \psi} = -\dot{t}. \end{aligned} \quad (3.16)$$

Inserting the classical energy into the equations of motion (3.16) one obtains:

$$\begin{aligned} A_- \left[ \sqrt{\frac{t(2S-t)}{r(2I-r)}}(I-r)2\cos(\psi-\varphi) + \frac{S}{2I} - \frac{1}{4IS}(2S-t) \right] &= \dot{\varphi}, \\ A_- \left[ \sqrt{\frac{r(2I-r)}{t(2S-t)}}(S-t)2\cos(\psi-\varphi) + \frac{I}{2S} - \frac{1}{4IS}(2I-r) \right] &= \dot{\psi}, \\ 2A_- \sqrt{rt(2I-r)(2S-t)} \sin(\psi - \phi) &= -\dot{r}, \\ -2A_- \sqrt{rt(2I-r)(2S-t)} \sin(\psi - \phi) &= -\dot{t}. \end{aligned} \quad (3.17)$$

Cancelling the time derivatives, the above equations lead to a set of equations defining the stationary points for the constant energy surface. The stationary angles are related by:

$$\overset{\circ}{\psi} = \overset{\circ}{\varphi} + \pi \quad (3.18)$$

while the stationary coordinates  $\overset{\circ}{r}$  and  $\overset{\circ}{t}$  are solutions of equations:

$$\begin{aligned} A_- \left[ -2\sqrt{\frac{t(2S-t)}{r(2I-r)}}(I-r) + \frac{S}{2I} - \frac{1}{4IS}(2S-t) \right] &= 0, \\ A_- \left[ -2\sqrt{\frac{r(2I-r)}{t(2S-t)}}(S-t) + \frac{I}{2S} - \frac{1}{4IS}(2I-r) \right] &= 0. \end{aligned} \quad (3.19)$$

It is worth mentioning that these solutions are stationary coordinates points for the constant energy function. Among them one depicts those which make the energy function minimum:

$$\mathcal{E}_1 = A_- \left[ -2\sqrt{rt(2I-r)(2S-t)} + \frac{I-1}{2S}t + \frac{S-1}{2I}r + \frac{rt}{4IS} \right]. \quad (3.20)$$

Note that equations of motion 3.17 are highly non-linear. However linearizing the left hand side by expanding it around the deepest minimum and keeping only the linear terms in the deviation,  $\varphi', \psi', r', t'$ , one obtains an integrable set of equations:

$$\begin{aligned}\{\mathcal{H}, q_1\} &= A_{11}p_1 + A_{12}p_2 = \dot{\bar{q}}_1, \\ \{\mathcal{H}, q_2\} &= A_{12}p_1 + A_{22}p_2 = \dot{\bar{q}}_2, \\ \{\mathcal{H}, p_1\} &= -B_{11}q_1 + B_{11}q_2 = \dot{\bar{p}}_1, \\ \{\mathcal{H}, p_2\} &= B_{11}q_1 - B_{11}q_2 = \dot{\bar{q}}_1.\end{aligned}\quad (3.21)$$

Here, the current point of the phase space was denoted by;

$$(q_1, q_2, p_1, p_2) = (\varphi', \psi', r', t') \quad (3.22)$$

while the analytical expressions of the involved coefficients,  $A_{11}, A_{12}, A_{22}, B_{11}$ , are given in Appendix A. For what follows it is useful to introduce the complex canonical coordinates:

$$\begin{aligned}\mathcal{B}^* &= \frac{q_1 + ip_1}{\sqrt{2}}, \quad \mathcal{B} = \frac{q_1 - ip_1}{\sqrt{2}}, \\ \mathcal{C}^* &= \frac{q_2 + ip_2}{\sqrt{2}}, \quad \mathcal{C} = \frac{q_2 - ip_2}{\sqrt{2}}.\end{aligned}\quad (3.23)$$

where  $i$  denotes the imaginary unit. The complex coordinates obey the following equations:

$$\begin{aligned}\{\mathcal{H}, \mathcal{B}^*\} &= \frac{i}{2} [\mathcal{B}^* (-A_{11} - B_{11}) + \mathcal{C}^* (-A_{12} + B_{11}) + \mathcal{B} (A_{11} - B_{11}) + \mathcal{C} (A_{12} + B_{11})], \\ \{\mathcal{H}, \mathcal{C}^*\} &= \frac{i}{2} [\mathcal{B}^* (-A_{12} + B_{11}) + \mathcal{C}^* (-A_{22} - B_{11}) + \mathcal{B} (A_{12} + B_{11}) + \mathcal{C} (A_{22} - B_{11})], \\ \{\mathcal{H}, \mathcal{B}\} &= \frac{i}{2} [\mathcal{B}^* (-A_{11} + B_{11}) + \mathcal{C}^* (-A_{12} - B_{11}) + \mathcal{B} (A_{11} + B_{11}) + \mathcal{C} (A_{12} - B_{11})], \\ \{\mathcal{H}, \mathcal{C}\} &= \frac{i}{2} [\mathcal{B}^* (-A_{12} - B_{11}) + \mathcal{C}^* (-A_{22} + B_{11}) + \mathcal{B} (A_{12} - B_{11}) + \mathcal{C} (A_{22} + B_{11})].\end{aligned}\quad (3.24)$$

Now we map the complex coordinates onto boson operators by using the correspondence:

$$(\mathcal{B}, \mathcal{B}^*, \mathcal{C}, \mathcal{C}^*) \rightarrow (b, b^\dagger, c, c^\dagger), \quad \{\cdot, \cdot\} \rightarrow \frac{1}{i} [\cdot, \cdot]. \quad (3.25)$$

Indeed, according to this mapping the newly introduced operators obey the boson-like commutation relations:

$$[b, b^\dagger] = 1, \quad [c, c^\dagger] = 1. \quad (3.26)$$

Moreover, the image of  $\mathcal{H}$  through this mapping is the Hamiltonian  $\hat{H}$  and Eqs. (3.24) lead to the equations of motion for the boson operators defined above. Using the resulting equations of motion for bosons, one can define the phonon operator

$$\Gamma_{s;IS}^\dagger = X_1 b^\dagger + X_2 c^\dagger - Y_1 b - Y_2 c, \quad (3.27)$$

such that the following equations are satisfied:

$$[\hat{H}, \Gamma_{s;IS}^\dagger] = \omega_s^{IS} \Gamma_{s;IS}^\dagger, \quad [\Gamma_{s;IS}, \Gamma_{s;IS}^\dagger] = 1. \quad (3.28)$$

These restrictions imply that the phonon amplitudes are determined by the equations:

$$\begin{pmatrix} \mathcal{A} & \mathcal{B} \\ -\mathcal{B} & -\mathcal{A} \end{pmatrix} \begin{pmatrix} X_1 \\ X_2 \\ Y_1 \\ Y_2 \end{pmatrix} = \omega_s^{IS} \begin{pmatrix} X_1 \\ X_2 \\ Y_1 \\ Y_2 \end{pmatrix},$$

$$X_1^2 + X_2^2 - Y_1^2 - Y_2^2 = 1. \quad (3.29)$$

Here  $\mathcal{A}$  and  $\mathcal{B}$  are  $2 \times 2$  matrices having the expressions:

$$\begin{aligned}\mathcal{A} &= \begin{pmatrix} \frac{1}{2}(A_{11} + B_{11}) & \frac{1}{2}(A_{12} - B_{11}) \\ \frac{1}{2}(A_{12} - B_{11}) & \frac{1}{2}(A_{22} + B_{11}) \end{pmatrix}, \\ \mathcal{B} &= \begin{pmatrix} \frac{1}{2}(-A_{11} + B_{11}) & \frac{1}{2}(-A_{12} - B_{11}) \\ \frac{1}{2}(-A_{12} - B_{11}) & \frac{1}{2}(-A_{22} + B_{11}) \end{pmatrix}. \end{aligned} \quad (3.30)$$

The index "s" suggests a semi-classical treatment. The solutions of these equations will be discussed in section 5.

#### IV. BOSON DESCRIPTION

##### A. The Dyson boson representation

The components of angular momenta written in terms of the conjugate classical coordinates look like:

$$\begin{aligned}I_+ &= \sqrt{r(2I-r)}e^{i\varphi}, \quad S_+ = \sqrt{t(2S-t)}e^{i\psi}, \\ I_- &= \sqrt{r(2I-r)}e^{-i\varphi}, \quad S_- = \sqrt{t(2S-t)}e^{-i\psi}, \\ I_3 &= r - I, \quad S_3 = t - S.\end{aligned} \quad (4.1)$$

Through a canonical transformation one obtains two other pairs of canonical conjugate classical coordinates:

$$\begin{aligned}\mathcal{C}_1 &= \frac{1}{\sqrt{2I}}\sqrt{r(2I-r)}e^{i\varphi}; \quad \mathcal{B}_1^* = \sqrt{2I}\sqrt{\frac{2I-r}{r}}e^{i\varphi}, \\ \mathcal{C}_2 &= \frac{1}{\sqrt{2S}}\sqrt{t(2S-t)}e^{i\psi}; \quad \mathcal{B}_2^* = \sqrt{2S}\sqrt{\frac{2S-t}{t}}e^{i\psi}.\end{aligned} \quad (4.2)$$

Indeed, it is easy to calculate the Poisson brackets of the conjugate coordinates. The result is:

$$\{\mathcal{B}_1^*, \mathcal{C}_1\} = i, \quad \{\mathcal{B}_2^*, \mathcal{C}_2\} = i, \quad (4.3)$$

where the symbol "i" denotes the imaginary unit. The classical coordinates are now quantized through the mapping:

$$\begin{aligned}\mathcal{C}_1 &\rightarrow C, \quad \mathcal{B}_1^* \rightarrow C^\dagger, \quad \{\cdot, \cdot\} \rightarrow -i[\cdot, \cdot], \\ \mathcal{C}_2 &\rightarrow D, \quad \mathcal{B}_2^* \rightarrow D^\dagger, \quad \{\cdot, \cdot\} \rightarrow -i[\cdot, \cdot].\end{aligned} \quad (4.4)$$

Through this mapping the classical angular momenta become the angular momenta operators:

$$\begin{aligned}\hat{I}_+ &= \sqrt{2IC}, \quad \hat{I}_- = \sqrt{2I}\left(C^\dagger - \frac{1}{2I}C^{\dagger 2}C\right), \quad \hat{I}_3 = I - C^\dagger C, \\ \hat{S}_+ &= \sqrt{2SD}, \quad \hat{S}_- = \sqrt{2S}\left(D^\dagger - \frac{1}{2S}D^{\dagger 2}D\right), \quad \hat{D}_3 = S - D^\dagger D.\end{aligned} \quad (4.5)$$

In the above equations we recognize the so called Dyson boson representation for angular momenta. Analogously, one can quantize any function defined on the classical phase space. In particular through quantization, the classical energy (3.14) becomes the Hamiltonian operator:

$$\begin{aligned}\hat{H} &= H_0 + A_- \left[ 2\sqrt{IS} (D^\dagger C + C^\dagger D) - \sqrt{\frac{S}{I}} C^{\dagger 2} CD - \sqrt{\frac{I}{S}} D^{\dagger 2} DC \right] + 2A_- (I - C^\dagger C) (S - D^\dagger D), \\ H_0 &= A_+ (I(I+1) + S(S+1)).\end{aligned} \quad (4.6)$$

If only the quadratic terms in bosons are retained from  $H$ , the result leads to the following equations of motion:

$$\begin{aligned}[H, C^\dagger] &= -2A_- SC^\dagger + 2A_- \sqrt{IS} D^\dagger, \\ [H, D^\dagger] &= 2A_- \sqrt{IS} C^\dagger - 2A_- ID^\dagger, \\ [H, C] &= 2A_- SC - 2A_- \sqrt{IS} D, \\ [H, D] &= -2A_- \sqrt{IS} C + 2A_- ID.\end{aligned} \quad (4.7)$$

Further we define the phonon operator:

$$\Gamma^\dagger = X_1 C^\dagger + X_2 D^\dagger - Y_1 C - Y_2 D, \quad (4.8)$$

such that the following restrictions are obeyed:

$$[H, \Gamma^\dagger] = \omega \Gamma^\dagger, \quad [\Gamma, \Gamma^\dagger] = 1. \quad (4.9)$$

The first equation, from above, yields a homogeneous system of equations for phonon amplitudes, whose compatibility restrictions determines the energy  $\omega$ :

$$\omega^2 \pm 2A_-(I + S)\omega = 0. \quad (4.10)$$

There are two non-vanishing solutions for  $\omega$ :

$$\omega = \mp 2A_-(I + S). \quad (4.11)$$

None of these solutions are acceptable here. Indeed, the first solution is negative, since as we shall see later  $A_- > 0$ , while in the second case the phonon operator does not satisfy the second equation (4.9). Due to these reasons we disregard this scenario.

The approximation described above can be improved by involving some contribution coming from the quartic boson terms of  $H$ , through the Bogoliubov transformation:

$$C^\dagger = U_1 \tilde{C}^\dagger - V_1 \tilde{C}, \quad D^\dagger = U_2 \tilde{D}^\dagger - V_2 \tilde{D}, \quad (4.12)$$

where the new operators are bosons and consequently the coefficients  $U$  and  $V$  obey the normalization conditions:

$$U_1^2 - V_1^2 = 1, \quad U_2^2 - V_2^2 = 1. \quad (4.13)$$

Writing the cubic operators in terms of the new bosons and then performing a normal ordering of the result and keeping only the linear terms one gets:

$$\begin{aligned} C^{\dagger 2} C &= 3U_1 V_1^2 \tilde{C}^\dagger - (U_1^2 V_1 + 2V_1^3) \tilde{C}, \\ D^{\dagger 2} D &= 3U_2 V_2^2 \tilde{D}^\dagger - (U_2^2 V_2 + 2V_2^3) \tilde{D}. \end{aligned} \quad (4.14)$$

The independent coefficients, say,  $V_1$  and  $V_2$  are fixed such that the cross terms  $\tilde{C}^\dagger \tilde{C}^\dagger + \tilde{C} \tilde{C}$  and  $\tilde{D}^\dagger \tilde{D}^\dagger + \tilde{D} \tilde{D}$  are cancelled. These restrictions lead to:

$$V_1^2 = I, \quad V_2^2 = S. \quad (4.15)$$

Inserting (4.14) into (4.6) one obtains a Hamiltonian that is quadratic in the new bosons. The salient feature of Dyson boson expansion is that it is a finite expansion. However, the drawback is that it does not preserve hermiticity, i.e. a hermitian operator becomes, after expansion, non-hermitian. This is the case of our Hamiltonian. Moreover, this is still valid even after the linearization. Despite the fact that the transformed Hamiltonian is non-hermitian, it has real eigenvalues [19]. Since it is not comfortable at all to diagonalize a non-Hermitian operator we prefer instead to use, from this point onward, the Hermitian operator:

$$\bar{H} = \frac{1}{2}(H + H^\dagger), \quad (4.16)$$

which admits the same eigenvalues as  $H$ . The equations of motion for the tilde operators are:

$$\begin{aligned} [\bar{H}, \tilde{C}^\dagger] &= a \tilde{D}^\dagger + b \tilde{D}, \\ [\bar{H}, \tilde{D}^\dagger] &= a \tilde{C}^\dagger + b \tilde{C}, \\ [\bar{H}, \tilde{C}] &= -b \tilde{D}^\dagger - a \tilde{D}, \\ [\bar{H}, \tilde{D}] &= -b \tilde{C}^\dagger - a \tilde{C}. \end{aligned} \quad (4.17)$$

where the following notations have been used:

$$\begin{aligned} a &= -\sqrt{I(I+1)S(S+1)} - IS - \frac{1}{2}(I+S), \\ b &= \frac{1}{2}\sqrt{I(I+1)}(2S+1) + \frac{1}{2}\sqrt{S(S+1)}(2I+1). \end{aligned} \quad (4.18)$$

The phonon operator

$$\Gamma_{b;IS}^\dagger = X_1 \tilde{C}^\dagger + X_2 \tilde{D}^\dagger - Y_1 \tilde{C} - Y_2 \tilde{D}. \quad (4.19)$$

is determined such that the following equations are fulfilled:

$$\begin{aligned} [\bar{H}, \Gamma_{b;IS}^\dagger] &= \omega_b^{IS} \Gamma_{b;IS}^\dagger, \\ [\Gamma_{b;IS}, \Gamma_{b;IS}^\dagger] &= 1. \end{aligned} \quad (4.20)$$

There exists only one solution of the above equations:

$$\begin{aligned} \omega_b^{IS} &= |a| A_- \\ X_1 &= \left(2 - \frac{b^2}{a^2}\right)^{-1/2}, \quad X_2 = -X_1, \\ Y_1 &= -\frac{b}{a} X_1, \quad Y_2 = 0. \end{aligned} \quad (4.21)$$

## V. MAGNETIC DIPOLE TRANSITIONS

The spherical components of magnetic dipole transition operator have the expressions:

$$M_{1\mu} = \sqrt{\frac{3}{4\pi}} (g_p I_{p\mu} + g_n I_{n\mu}), \quad (5.1)$$

where  $g_p, g_n$  denote the protons and neutrons gyromagnetic factor, respectively. Written in terms of the angular momenta  $\vec{I}$  and  $\vec{S}$  the transition operator becomes:

$$M_{1\mu} = \sqrt{\frac{3}{4\pi}} (g_+ I_\mu + g_- S_\mu), \quad (5.2)$$

with the notations:

$$g_\pm = \frac{g_p \pm g_n}{2}. \quad (5.3)$$

### A. Semi-classical description

The states  $|I^+\rangle$  forming the band (I,1) are vacuum states for the phonon operator (3.27) corresponding to the energy  $\omega_s^{I,1}$ . Due to this remark we use the notation  $|0\rangle_{s,I}$  for the state  $|I^+\rangle$ . One can easily check that the phonon operator is a tensor of rank 1.

We are interested in calculating the transition between the states  $|o\rangle_{s,I}$  and  $|(1+1)^+, \mu\rangle = \Gamma_{1,\mu}^\dagger |0\rangle_{s,I}$ . One can easily check that in order to calculate the matrix elements characterizing the transition  $|1^+\rangle \rightarrow |(I+1)^+\rangle$  we have first to expand, in the first order, the angular momenta components (4.1) around the energy function minimum and then quantize the deviations according to the procedure described in Section 3. Results for the first phonon state

decay are as follows:

$$\begin{aligned}
{}_{s,I}\langle 0|I_{+1}\Gamma_{1,-1}^\dagger|0\rangle_{s,I} &= \frac{-i}{2} \left[ \frac{I - \overset{\circ}{r}}{\sqrt{\overset{\circ}{r}(2I - \overset{\circ}{r})}} (Y_1 - X_1) - \sqrt{\overset{\circ}{r}(2I - \overset{\circ}{r})} (Y_1 + X_1) \right], \\
{}_{s,I}\langle 0|I_{-1}\Gamma_{1,+1}^\dagger|0\rangle_{s,I} &= \frac{-i}{2} \left[ \frac{I - \overset{\circ}{r}}{\sqrt{\overset{\circ}{r}(2I - \overset{\circ}{r})}} (Y_1 - X_1) + \sqrt{\overset{\circ}{r}(2I - \overset{\circ}{r})} (Y_{11} + X_{11}) \right], \\
{}_{s,I}\langle 0|I_0\Gamma_{1,0}^\dagger|0\rangle_{s,I} &= \frac{i}{\sqrt{2}} (X_1 - Y_1), \\
{}_{s,I}\langle 0|S_{+1}\Gamma_{1,-1}^\dagger|0\rangle_{s,I} &= \frac{-i}{2} \left[ \frac{S - \overset{\circ}{t}}{\sqrt{\overset{\circ}{t}(2S - \overset{\circ}{t})}} (Y_2 - X_2) - \sqrt{\overset{\circ}{t}(2S - \overset{\circ}{t})} (Y_2 + X_2) \right], \\
{}_{s,I}\langle 0|S_{-1}\Gamma_{1,+1}^\dagger|0\rangle_{s,I} &= \frac{-i}{2} \left[ \frac{S - \overset{\circ}{t}}{\sqrt{\overset{\circ}{t}(2S - \overset{\circ}{t})}} (Y_{21} - X_{21}) + \sqrt{\overset{\circ}{t}(2S - \overset{\circ}{t})} (Y_2 + X_2) \right], \\
{}_{s,I}\langle 0|S_0\Gamma_{1,0}^\dagger|0\rangle_{s,I} - [s, I] &= \frac{i}{\sqrt{2}} (X_2 - Y_2).
\end{aligned} \tag{5.4}$$

Using these matrix elements, the reduced probability for the M1 dipole transition from a I state of the ground band to the  $(I+1)^+$  state of the excited band, is readily obtained

$$B(M1; I^+ \rightarrow (I+1)^+) = \sum_\mu |{}_{s,I}\langle 0|\Gamma_{s,I1,\mu} M_1 \mu |0\rangle_{s,I}|^2. \tag{5.5}$$

## B. The full Dyson boson expansion

The linearized boson expansions associated to the a.m. components are:

$$\begin{aligned}
I_+^D &= \sqrt{2I} \left( U_1 \tilde{C} - V_1 \tilde{C}^\dagger \right), \\
I_-^D &= \sqrt{2I} \left[ \left( U_1 - \frac{3}{2I} U_1 V_1^2 \right) \tilde{C}^\dagger + \left( -V_1 + \frac{1}{2I} (U_1^2 V_1 + 2V_1^3) \right) \tilde{C} \right], \\
S_+^D &= \sqrt{2S} \left( U_2 \tilde{D} - V_2 \tilde{D}^\dagger \right), \\
S_-^D &= \sqrt{2S} \left[ \left( U_2 - \frac{3}{2S} U_2 V_2^2 \right) \tilde{D}^\dagger + \left( -V_2 + \frac{1}{2S} (U_2 V_2 + 2V_2^3) \right) \tilde{D} \right].
\end{aligned} \tag{5.6}$$

We note that the hermiticity property is broken, i.e.  $(I_+^D)^\dagger \neq I_-^D$  and  $(S_+^D)^\dagger \neq S_-^D$ .

To calculate the M1 transition probability for the case when the full Dyson boson expansion is used for angular momenta, we need the following matrix element:

$$\begin{aligned}
{}_{b,I}\langle 0|I_{+1}^D\Gamma_{1,-1}^\dagger|0\rangle_{b,I} &= -\sqrt{I} (U_1 X_1 - V_1 Y_1), \\
{}_{b,I}\langle 0|I_{-1}^D\Gamma_{1,+1}^\dagger|0\rangle_{b,I} &= \sqrt{I} \left[ -V_1 X_1 + U_1 Y_1 - \frac{1}{2I} (3U_1 V_1^2 Y_1 - (U_1^2 V_1 + 2V_1^3) X_1) \right], \\
{}_{b,I}\langle 0|S_{+1}^D\Gamma_{1,-1}^\dagger|0\rangle_{b,I} &= -\sqrt{S} (U_2 X_2 - V_2 Y_2), \\
{}_{b,I}\langle 0|S_{-1}^D\Gamma_{1,+1}^\dagger|0\rangle_{b,I} &= \sqrt{S} \left[ -V_2 X_2 + U_2 Y_2 - \frac{1}{2S} (3U_2 V_2^2 Y_2 - (U_2^2 V_2 + 2V_2^3) X_2) \right].
\end{aligned} \tag{5.7}$$

Here, the notations  $I_{\pm 1}^D$  and  $S_{\pm 1}^D$  are used for the spherical components of the angular momenta  $\vec{I}$  and  $\vec{S}$ , respectively.

Using these matrix elements the reduced transition probability is readily obtained

$$B(M1; I^+ \rightarrow (I+1)^+) = \sum_\mu |{}_{b,I}\langle 0|\Gamma_{b,I1,\mu} M_1 \mu |0\rangle_{b,I}|^2. \tag{5.8}$$

## VI. NUMERICAL ANALYSIS

The model Hamiltonian involves two parameters; these are the moments of inertia for protons and neutrons respectively. At their turn they define the parameters  $A_+$  and  $A_-$  which are actually used to describe both the energies and the magnetic dipole transitions. The experimental value for the moment of inertia of nuclei can be approximated by the compact formula [20]

$$\mathcal{J}_{exp} = \frac{\beta^2 A^{7/3}}{400} [\hbar^2 MeV^{-1}]. \quad (6.1)$$

where  $\beta$  denotes the nuclear quadrupole deformation and  $A$  is the nuclear mass number. This is larger than the irrotational moment of inertia by a factor  $2 \div 3$ . In order to keep close to the hydrodynamic picture we quenched the moment of inertia given by Eq. (6.1), by a factor of 2.5. The result is multiplied successively by the factors  $Z/A$  and  $N/A$  as to obtain the proton and neutron moment of inertia, respectively. The obvious notations for nuclear charge ( $Z$ ) and neutron number ( $N$ ) are used. Application concerns the isotope  $^{156}\text{Gd}$  for which  $\beta=0.266$  [21] and  $A=156$ . Thus one obtains:

$$A_+ = 0.05574\text{MeV}, A_- = 0.01\text{MeV}. \quad (6.2)$$

The stationary values for the coordinates  $r, t$ , are obtained by solving the equations (3.19). Since the corresponding Hessian is positive the solutions define the minimum of the energy function. Results are collected in Table 1 for two sets of pairs  $(I, S)$ , namely  $(I, 1)$  with  $I=1, 2, 3, \dots, 10$  and  $(1, S)$  with  $S=1, 2, 3, \dots, 10$ . The minima of the energy  $\mathcal{E}_1$ , as a function of the coordinates  $r$  and  $t$ , are depicted in Fig. 1 through a contour plot for four representative pairs of angular momenta,  $(I, S)$ . Note a certain symmetry in Table 1. Indeed,  $(\overset{\circ}{r}, \overset{\circ}{t})$  for the band  $(I, 1)$  are equal with  $(\overset{\circ}{t}, \overset{\circ}{r})$  for  $(1, S)$ . This degeneracy reflects the invariance of the energy function for the interchange of  $I$  with  $S$  and  $r$  with  $t$

As for the stationary angles they satisfy the relation  $\overset{\circ}{\psi} - \overset{\circ}{\varphi} = \pi$ . We made the option for  $\overset{\circ}{\psi} = \pi$  and  $\overset{\circ}{\varphi} = 0$ .

These data are further used to calculate the wobbling frequency, by solving the RPA-like equation (3.29) ,for the semi classical framework and (4.21) for the boson description. Wobbling frequencies, thus obtained, are employed to calculate the energies in the ground band and the one-phonon excited band:

$$\begin{aligned} E_{s,1}^{I1} &= A_+ [I(I+1) + S(S+1)] + \frac{1}{2} \omega_s^{IS}, \\ E_{s,2}^{I+1,1} &= A_+ [I(I+1) + S(S+1)] + \frac{3}{2} \omega_s^{IS}, \\ E_{b,1}^{I1} &= A_+ [I(I+1) + S(S+1)] + \frac{1}{2} \omega_b^{IS}, \\ E_{b,2}^{I+1,1} &= A_+ [I(I+1) + S(S+1)] + \frac{3}{2} \omega_b^{IS}. \end{aligned} \quad (6.3)$$

(I,S)	$\overset{\circ}{r}$	$\overset{\circ}{t}$	(1,S)	$\overset{\circ}{r}$	$\overset{\circ}{t}$
(1,1)	0.888889	0.888889	(1,1)	0.888889	0.888889
(2,1)	1.89609	0.81856	(1,2)	0.81856	1.89609
(3,1)	2.89829	0.79726	(1,3)	0.79726	2.89829
(4,1)	3.89935	0.786972	(1,4)	0.786972	3.89935
(5,1)	4.89998	0.780911	(1,5)	0.780911	4.89998
(6,1)	5.90039	0.776915	(1,6)	0.776915	5.90039
(7,1)	6.90068	0.774083	(1,7)	0.774083	6.90068
(8,1)	7.9009	0.771971	(1,8)	0.771971	.9009
(9,1)	8.90107	0.770335	(1,9)	0.770335	8.90107
(10,1)	9.9012	0.769031	(1,10)	0.769031	9.9012

TABLE I: The coordinates  $r$  and  $t$  for the minimum point of the energy surface.

The wobbling frequencies and the energies of the ground and one-phonon excited bands as obtained from the semi-classical and boson descriptions respectively, are presented in Table 2 and illustrated in Fig. 2. We note that predictions of the two formalisms are close to each other.

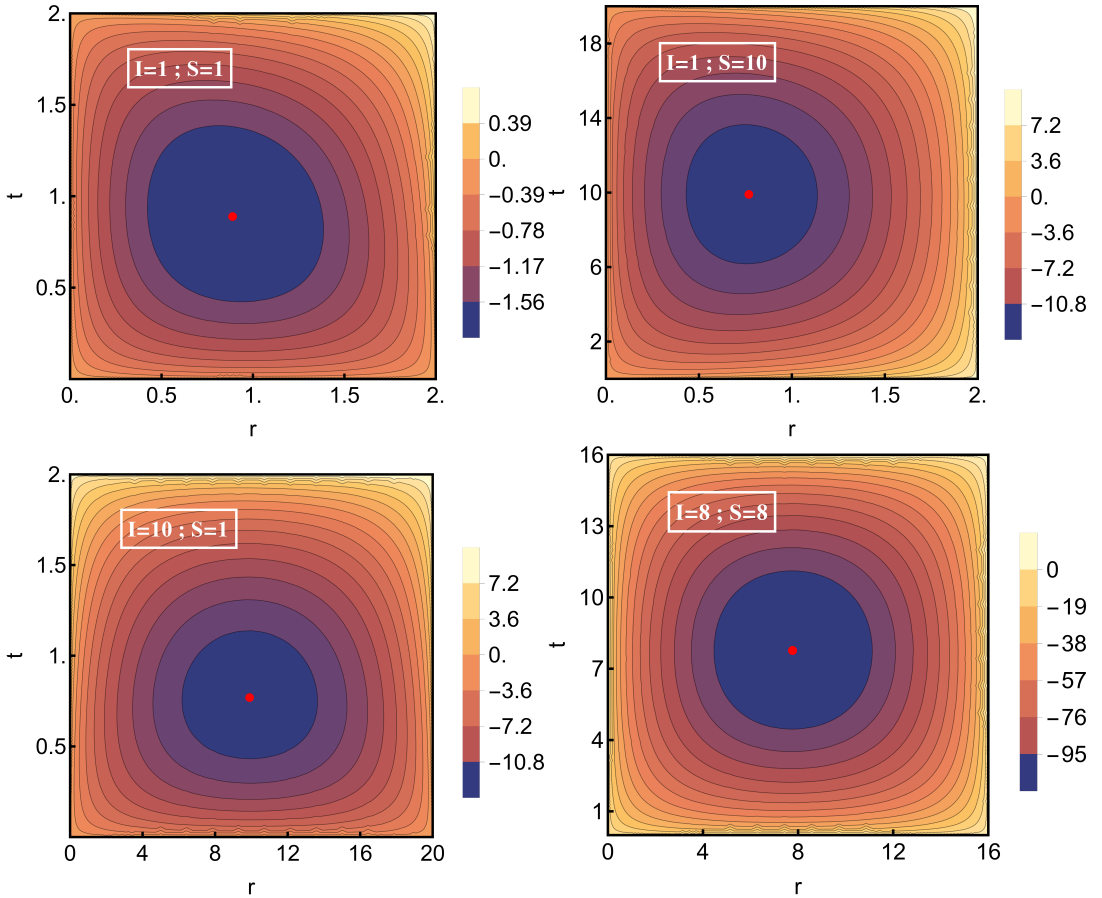


FIG. 1: Contour plots for four angular momenta pairs,  $(I, S)$ , and the energy function (3.20) taken for  $\psi - \phi = \pi$ .

$(I, S)$	$\omega_s^{I1}$ [MeV]	$\omega_b^{I1}$ [MeV]	$E_{s1}^{I1}$ [MeV]	$E_{b1}^{I1}$ [MeV]	$E_{s2}^{I1}$ [MeV]	$E_{b2}^{I1}$ [MeV]
(1,1)	0.02667	0.04000	0.23629	0.24296	-	-
(2,1)	0.04421	0.06964	0.46803	0.48074	0.26296	0.55038
(3,1)	0.06366	0.09899	0.81219	0.82985	0.51224	0.92884
(4,1)	0.08368	0.12825	1.26812	1.29040	0.87585	1.41865
(5,1)	0.10393	0.15746	1.83564	1.86241	1.35179	2.01987
(6,1)	0.12430	0.18665	2.51471	2.54589	1.93957	2.73254
(7,1)	0.14474	0.21583	3.30529	3.34083	2.63901	3.55667
(8,1)	0.16523	0.24500	4.20737	4.24726	3.45003	4.49226
(9,1)	0.18574	0.27416	5.2209	5.26516	4.37260	5.53933
(10,1)	0.20628	0.30332	6.34602	6.39454	5.40669	6.69787

TABLE II: Wobbling frequencies and energies for the first (ground) and second (one-phonon excited) band are given in units of MeV for  $I$  running from 1 to 10.

The amplitudes of the phonon operator are used now to calculate the reduced probability to perform the  $M1$  transition  $I^+ \rightarrow (I + 1)^+$ . Aiming at this goal the raising and lowering operators  $I_\pm$  and  $S_\pm$  are expressed as linear combination of the boson operators composing the dipole phonon operator. Results are given in Table III. From there it can be seen that the  $B(M1)$  values are increasing with respect to  $I$ . Comparing the predictions of the two formalisms one remarks that boson expansion results are by a factor of 4 ÷ 10 larger than those corresponding to the semi-classical treatment. The reason is that the linearization procedures for the transition operators used in the two cases are different. It seems that Bogoliubov transformation affects the phonon amplitudes in a more efficient way.

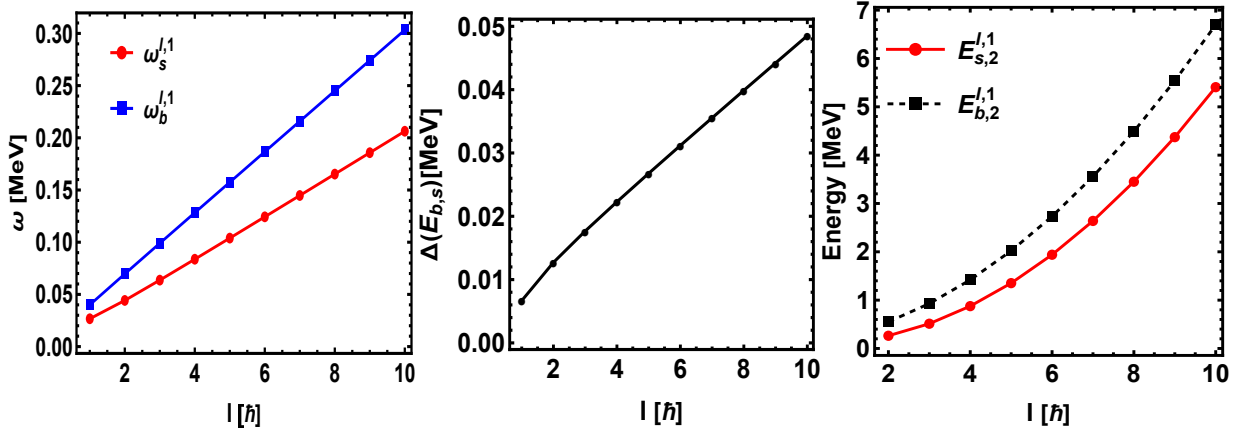


FIG. 2: Semi-classical and boson wobbling frequencies( $\omega_s^{I,1}$  and  $\omega_b^{I,1}$ ) and energy differences for the ground bands ( $\Delta E_{b,s} = E_{b,1}^{I,1} - E_{s,1}^{I,1}$ ) and the first one phonon excited bands ( $E_{s,2}^{I,1}$  and  $E_{b,2}^{I,1}$ )

I	$B(M1; I^+ \rightarrow (I+1)^+) [\mu_N^2]$	
	semi-classic	Dyson boson
1	0.01168	0.04972
2	0.03812	0.15425
3	0.06453	0.31536
4	0.09034	0.53300
5	0.11586	0.80717
6	0.14123	1.13784
7	0.16652	1.52502
8	0.19177	1.96871
9	0.21699	2.46891

TABLE III: The  $B(M1)$  values for the dipole transitions  $I^+ \rightarrow (i+1)^+$  are given for  $I=1,2,3,\dots,9$ , in units of  $\mu_N^2$ .

A natural question arises about the nature of these states. Are they scissors or shears modes? To answer this question one has to calculate the angle between  $\vec{I}_p$  and  $\vec{I}_n$ . In order to touch this goal one needs to calculate the angle between  $\vec{I}$  and  $\vec{S}$ . The value for this angle is obtained by solving the equation:

$$\cos(\theta_{IS}) = \frac{\vec{I} \cdot \vec{S}}{|\vec{I}| |\vec{S}|} = \frac{F(I, S, \overset{\circ}{r}, \overset{\circ}{t})}{\sqrt{I(I+1)S(S+1)}}, \quad (6.4)$$

where the function F has the expression:

$$F(I, S, \overset{\circ}{r}, \overset{\circ}{t}) = \frac{1}{2} \left[ -2\sqrt{\overset{\circ}{r}\overset{\circ}{t}(2I-1)(2S-1)} + (I-1)(S-1) \right] + \frac{I-1}{2S} \overset{\circ}{r} + \frac{S-1}{2I} \overset{\circ}{r} + \frac{\overset{\circ}{r}\overset{\circ}{r}}{4IS}. \quad (6.5)$$

As for the angle between the angular momenta  $\vec{I}_p$  and  $\vec{I}_n$ . this is the solution of equation:

$$\begin{aligned} \cos(\theta_{pn}) &= \frac{\vec{I}_p \cdot \vec{I}_n}{|\vec{I}_p| |\vec{I}_n|} \\ &= \frac{I(I+1) - S(S+1)}{\sqrt{[I(I+1) + S(S+1) + 2F(I, S, \overset{\circ}{r}, \overset{\circ}{t})][I(I+1) + S(S+1) - 2F(I, S, \overset{\circ}{r}, \overset{\circ}{t})]}}. \end{aligned} \quad (6.6)$$

Another relevant aspect is the contribution of proton and neutron angular momenta to the total angular momenta

$I$  and  $S$  as determined by the following relations:

$$\begin{aligned} I_p &= \frac{1}{2}|\vec{I} + \vec{S}| = \frac{1}{2}\sqrt{I(I+1) + S(S+1) + 2F(I, S, \overset{\circ}{r}, \overset{\circ}{t})}, \\ I_n &= \frac{1}{2}|\vec{I} - \vec{S}| = \frac{1}{2}\sqrt{I(I+1) + S(S+1) - 2F(I, S, \overset{\circ}{r}, \overset{\circ}{t})}. \end{aligned} \quad (6.7)$$

Results of this analysis are shown in Table IV. From there we see that the angle between  $\vec{I}$  and  $\vec{S}$  vary slowly around  $120^\circ$  while that between  $\vec{I}_p$  and  $\vec{I}_n$  is decreasing from  $90^\circ$  to  $13^\circ$ . One notices that for low  $I$  the states  $(I,1)$  have shears character while for large  $I$  due to the alignment of proton and neutron angular momenta, the states tend to have a scissors nature. This is different from the prediction of two rotor model where the state  $1^+$  has a scissors character. As for the angular momentum composition in a given state, the result is that  $\langle I_n \rangle > \langle I_p \rangle$ . This ordering is determined by the fact the neutron moment of inertia is larger than the proton one. On the last row of Table IV we listed the results of  $I = 8$  and  $S = 8$ . This state is also of shears type, as any other state with  $I = S$ . Otherwise the other features mentioned for the  $(I, 1)$  states are still valid. Since the rotational energy is large in this case the wobbling frequencies and the band energies are large as well. This aspect is outlined in the following table:

$$\begin{aligned} \omega_s^{81} &= 0.305, \text{ MeV} \\ E_{s,1}^{81} &= 8.179 \text{ MeV}, \quad E_{s,2}^{91} = 8.484 \text{ MeV}, \\ B(M1; 8^+ \rightarrow 9^+) &= 0.228\mu_N^2, \\ \omega_b^{81} &= 1.44, \text{ MeV} \\ E_{b,1}^{81} &= 8.746 \text{ MeV}, \quad E_{b,2}^{91} = 10.186 \text{ MeV}, \\ B(M1; 8^+ \rightarrow 9^+) &= 1.936\mu_N^2. \end{aligned} \quad (6.8)$$

Obviously, results for energy strongly depend on the proton and neutron moment of inertia. To stress on this we give

(I,S)	$\angle(\vec{I}, \vec{S})$ [°]	$\angle(\vec{I}_p, \vec{I}_n)$ [°]	$\langle I_p \rangle$ [h]	$\langle I_p \rangle$ [h]
(1,1)	116.388	90.000	0.745	1.202
(2,1)	118.680	56.651	1.081	1.683
(3,1)	119.887	40.348	1.510	2.173
(4,1)	120.614	31.165	1.972	2.667
(5,1)	121.099	25.350	2.449	3.162
(6,1)	121.445	21.353	2.934	3.660
(7,1)	121.705	18.442	3.423	4.157
(8,1)	121.906	16.228	3.915	4.655
(9,1)	122.067	14.488	4.409	5.154
(10,1)	122.199	13.085	4.904	5.653
(8,8)	119.873	90.000	4.251	7.344

TABLE IV: Angles for the pairs of vectors  $(\vec{I}, \vec{S})$  and  $(\vec{I}_p, \vec{I}_n)$ , the average proton and neutron angular momenta corresponding to a state of angular momenta  $I$  and  $S = 1$ , respectively.

an example where the nuclear moment of inertia is chosen such that the energy of the  $K=2$  state  $2^+$ , i.e. the head state of the band  $\gamma$  [22], is reproduced. Thus, one obtains  $A_- = 0.10775\hbar^2 \text{ MeV}^{-1}$  and  $A_+ = 0.60034\hbar^2 \text{ MeV}^{-1}$ . Results for wobbling energies and the first energy levels of the ground and excited band are synthesized in the following array:

$$\begin{aligned} \omega_s^{11} &= 0.287, \text{ MeV} \\ E_{s,1}^{11} &= 2.545 \text{ MeV}, \quad E_{s,2}^{21} = 2.83 \text{ MeV}, \\ B(M1; 1^+ \rightarrow 2^+) &= 0.012\mu_N^2, \\ \omega_b^{11} &= 0.431 \text{ MeV}, \\ E_{b,1}^{11} &= 2.617 \text{ MeV}, \quad E_{b,2}^{21} = 3.048 \text{ MeV}, \\ B(M1; 1^+ \rightarrow 2^+) &= 0.05\mu_N^2. \end{aligned} \quad (6.9)$$

It is worth noting that energies for the state  $(I=1, S=1)$  obtained within the semi-classical and boson expansion formalisms, are not far from the energy of the scissors mode, which is equal to 3.075 MeV [8]. Amazingly is the fact

that the predicted energy for the first state of the excited phonon band (3.048 MeV), by the boson expansion method, almost coincides with the scissors mode energy. However the mentioned boson prediction is a state of total angular momentum  $I=2$ . This is caused by that the phonon operator, which creates the state  $2^+$ , admits the state  $1^+$  as vacuum state.

As we already mentioned there exists a band (1,I) which is degenerate with the band (I,1). The degeneracy is caused by the invariance of the Hamiltonian to the interchange of  $I$  with  $S$  and  $r$  with  $t$ . Note that the mentioned transformation is equivalent with changing the sign of  $\vec{I}_n$  which actually is a chiral transformation. The degeneracy of the mentioned bands can be lifted up by adding to the model Hamiltonian a term which breaks the chiral symmetry. An example of such a term is:

$$V = \kappa \vec{I}_p \cdot \vec{I}_n. \quad (6.10)$$

It can be checked that this induces an energy split

$$\Delta E_I = 2I(I+1) - 4. \quad (6.11)$$

For an ad hoc choice of  $\kappa=3$  keV, the above split ranges from 24 keV for  $I=2$  to 648 keV for  $I=10$ . The non-degenerate bands (I,1) and (1,I) exhibit the features of a chiral twin doublet.

Concluding this section, we formulated two formalism in order to interpret the semi-classical features of the two rotor system. We pointed out the existence of two degenerate bands labeled by (I,1) and (1,S) respectively. Also, we calculated the properties of the one phonon excited band. We found out that wobbling motion is not the exclusive virtue of the triaxial rotor system but also for a two axial symmetric rotors.

## VII. APPENDIX A

The expressions for the coefficients involved in the linearized equations of motion are as follows:

$$\begin{aligned} A_{11} &= 2A_- I^2 \frac{\sqrt{t(2S-t)}}{(r(2I-r))^{3/2}} \left| \begin{array}{l} r = \overset{\circ}{r} \\ t = \overset{\circ}{t} \end{array} \right. , \\ A_{12} &= A_- \left[ \frac{1}{4IS} - 2 \frac{(I-r)(S-t)}{\sqrt{rt(2I-r)(2S-t)}} \right] \left| \begin{array}{l} r = \overset{\circ}{r} \\ t = \overset{\circ}{t} \end{array} \right. , \\ A_{22} &= 2A_- S^2 \frac{\sqrt{r(2I-r)}}{(t(2S-t))^{3/2}} \left| \begin{array}{l} r = \overset{\circ}{r} \\ t = \overset{\circ}{t} \end{array} \right. , \\ B_{11} &= 2A_- \sqrt{rt(2I-r)(2S-t)} \left| \begin{array}{l} r = \overset{\circ}{r} \\ t = \overset{\circ}{t} \end{array} \right. \end{aligned} \quad (A.1)$$

## VIII. CONCLUSIONS

A two axial symmetric rotor Hamiltonian is alternatively treated semi-classically, via a Time Dependent Variational Principle, and by a Dyson boson expansion method. In both cases the linearized equations of motion lead to dispersion equations for the wobbling frequencies. A ground band is built up with the states having the zero-point energies. The corresponding phonon operators are exciting a second band. The energies of the two bands are compared with each others. The phonon amplitudes are used to calculate the  $B(M1)$  values regarding the reduced probability for the transition from the state  $I$  from the ground band to the state  $I+1$  from the excited band. Calculations are

performed using Z=64 and N=92, i.e. data for  $^{156}$  Gd. The states from the two bands have a shears character in the beginning of the bands and acquire a scissors feature by increasing the angular momentum, due to the alignment effect. The neutron angular momentum contribution to the total angular momentum prevails over the proton one. It is shown that fixing the moment of inertia by fitting the energy of the K=2 state  $2_{\gamma}^{+}$ , the energy of the the  $2^{+}$  from the excited band is very close to the energy of the scissors dipole state,  $1^{+}$ . The ground band (I,I) is degenerate with the band (1,I) due to the chiral symmetry. Adding an interaction which breaks the mentioned symmetry the degeneracy is lifted up and consequently a chiral twin band doublet shows up.

In conclusion, the two-rotor Hamiltonian successfully captures both wobbling and chiral features of nuclear systems. Experimental data in this context would provide valuable motivation for further investigations.

- [1] W. Greiner, Phys. Rev. Lett. **14**, 599 (1965); W. Greiner, Nucl. Phys. **80**, 417 (1966); A. Faessler, W. Greiner, Z. Phys. **179**, 343 (1964)
- [2] A. Faessler, Nucl. Phys. **85**, 417 (1966)
- [3] V. Maruhn-Rezwani, W. Greiner, J.A. Maruhn, Phys. Lett **57**, 109 (1975)
- [4] S.I. Gabrakov, A.A. Kuliev, N.I. Pyatov, Yad. Fiz. **12**, 82 (1970); (Sov. J. Nucl. Phys. **12**, 44 (1971)); S.I. Gabrakov, A.A. Kuliev, N.I. Pyatov, D.I. Salamov, H. Schulz, Nucl. Phys. A **182**, 625 (1972)
- [5] A.A. Kuliev, N.I. Pyatov, Yad. Fiz. **20**, 297 (1974)
- [6] T. Suzuki, D.J. Rowe, Nucl. Phys. A **289**, 461 (1977)
- [7] N. Lo Iudice, F. Palumbo, Phys. Rev. Lett. **74**, 1046 (1978); G. De Franceschi, F. Palumbo, N. Lo Iudice, Phys. Rev. C **29**, 1496 (1984)
- [8] D. Bohle, A. Richter, W. Steffen, A.E.L. Dieprink, N. Lo Iudice, F. Palumbo, O. Scholten, Phys. Lett. B **137**, 27 (1983)
- [9] U.E.P. Berg, C. Blassing, J. Drexler, R.D. Heil, U. Kneissle, W. Naatz, H. Ratzek, S. Schennach, R. Stock, T. Weber, H. Wickert, B. Fusher, H. Hollik, D. Kollewe, Phys. Lett. B **149**, 59 (1984)
- [10] F. Iachello, Nucl. Phys. **A358**, 89c (1981)
- [11] A. A. Raduta, Amand Faessler and V. Ceausescu, Phys. Rev. C**36**, 2111 (1987).
- [12] N. Lo Iudice, A. A. Raduta and D. S. Delion, Phys. Rev. C **50**, 127 (1994).
- [13] A. A. Raduta, N. Lo Iudice, Z. Fur Phys. A **334** 403 (1989).
- [14] A. A. Raduta and D. S. Delion, Nucl. Phys. **A513**, 11 (1990).
- [15] A. Richter, Nucl. A. Phys. **507**, 99c (1990); A **522**, 139c (1991); A **553**, 417 (1993). Prog. Part. Nucl. Phys. **34**, 261 (1995)
- [16] N. Lo Iudice, Prog. Part. Phys. **34**, 309 (1995)
- [17] D. Zawischa, J. Phys. G**24**, 683, (1998).
- [18] A. A. Raduta, R. Poenaru and L. Gr. Ixaru, Phys. Rev. C **96**, 054320 (2017).
- [19] T.Oguchi, Prog. Th. Phys.**26**, 26, 721 (1961).
- [20] P. Ring and P. Scuk, in The Nuclear Many-Body Problem, Springer- Verlag, Berlin, Heidelberg, New York, p. 19.
- [21] G. A. Lalazissis, S. Raman, P. Ring, Atomic Data and Nuclear Data Tables **71**, 1– 40 (1999).
- [22] M. Finger, T. I.Krakova, I Pricharzka and J. Ferenzei, Phys. Scr. **27**,8 (1983).